Retraction

MEDICAL SCIENCES

Retraction for "Impaired lipid metabolism by age-dependent DNA methylation alterations accelerates aging," by Xin Li, Jiaqiang Wang, Leyun Wang, Guihai Feng, Gen Li, Meixin Yu, Yufei Li, Chao Liu, Xuewei Yuan, Guangxi Zang, Zhihuan Li, Ling Zhao, Hong Ouyang, Qingli Quan, Guangyu Wang, Charlotte Zhang, Oulan Li, Junkai Xiang, Jian-Kang Zhu, Wei Li, Qi Zhou, and Kang Zhang, which was first published February 6, 2020; 10.1073/pnas.1919403117 (*Proc. Natl. Acad. Sci. U.S.A.* **117**, 4328–4336).

The authors wish to note the following: "It came to our attention after publication that the fundus images in Fig. 3*E* and *SI Appendix*, Fig. S4*C* of our PNAS article were a duplication of the photos in a recent *Aging Cell* article (1). These photographs were generated by Dr. Daniel Chen and Dr. Dorota Skowronska-Krawczyk in the course of conducting research exploring the effects of Elovl2 deficiency in the mouse eye at Dr. Kang Zhang's laboratory at University of California San Diego. In the same time period, the authors of the PNAS paper were working at the same laboratory exploring the effects of the Elovl2 loss in the entire mouse body. While the two groups of researchers were working concurrently at Dr. Zhang's University of California San Diego laboratory, the fundus photographs were inadvertently misidentified and mixed in with materials developed for the Elovl2 mouse strain in the PNAS paper, during the process of data organization and presentation. The similarities in genetic properties between the Elovl2 mouse strains contributed to the confusion and subsequent mix-up.

"We apologize to the scientific community for this inadvertent error. Despite the fact that this is an honest mistake and the inclusion of the erroneously misidentified photos did not affect the conclusions of the PNAS article nor the validity of the remaining data and findings in the paper, including all of the data generated from the laboratories of Drs. Qi Zhou, Wei Li, and Jian-Kang Zhu, who are unaccountable for this inadvertent error, we believe that a retraction is appropriate to prevent confusion among the scientific community. The affiliation of Dr. Xin Li needs to be corrected as University of California, San Diego, rather than Whitehead Institute for Biomedical Research."

1. D. Chen, D. L. Chao, L. Rocha, M. Kolar, V. A. N. Huu, M. Krawczyk, M. Dasyani, T. Wang, M. Jafari, M. Jabari, K. D. Ross, A. Saghatelian, B. A. Hamilton, K. Zhang, D. Skowronska-Krawczyk, The lipid elongation enzyme ELOVL2 is a molecular regulator of aging in the retina. *Aging Cell* 19, e13100 (2020).

First published March 27, 2020.

www.pnas.org/cgi/doi/10.1073/pnas.2005286117

See Retraction Published March 27, 2020

Impaired lipid metabolism by age-dependent DNA methylation alterations accelerates aging

Xin Li[a,1], Jiaqiang Wang[b,1], Leyun Wang[b,1], Guihai Feng[b,1], Gen Li[c,d,1], Meixin Yu[c,d], Yufei Li[b], Chao Liu[b], Xuewei Yuan[b], Guangxi Zang[e], Zhihuan Li[e], Ling Zhao[f], Hong Ouyang[f], Qingli Quan[c,d], Guangyu Wang[g], Charlotte Zhang[e], Oulan Li[e], Junkai Xiang[d], Jian-Kang Zhu[h,i,2], Wei Li[b,2], Qi Zhou[b,2], and Kang Zhang[d,2]

[a]Whitehead Institute for Biomedical Research, Cambridge, MA 02142; [b]State Key Laboratory of Stem Cell and Reproductive Biology, Institute of Zoology, Chinese Academy of Sciences, 100101 Beijing, China; [c]Center for Genetic Disease Diagnosis, Guangzhou Women and Children Medical Center, 510005 Guangzhou, China; [d]Faculty of Medicine, Macau University of Science and Technology, Tapai, 999078 Macau, China; [e]Department of Bioinformatics, Guangzhou Regenerative Medicine and Health Guangdong Laboratory, 510005 Guangzhou, China; [f]State Key Laboratory of Ophthalmology, Zhongshan Ophthalmic Center, Sun Yat-sen University, 510005 Guangzhou, China; [g]Department of Computer Science and Technology, Tsinghua University, 100084 Beijing, China; [h]Shanghai Center for Plant Stress Biology, Shanghai Institute for Biological Sciences, Chinese Academy of Sciences, 210602 Shanghai, China; and [i]Department of Horticulture and Landscape Architecture, Purdue University, West Lafayette, IN 47907

Contributed by Jian-Kang Zhu, December 17, 2019 (sent for review November 6, 2019; reviewed by Stephan Beck, Hongkui Deng, and Andrew E. Teschendorff)

Epigenetic alterations and metabolic dysfunction are two hallmarks of aging. However, the mechanism of how their interaction regulates aging, particularly in mammals, remains largely unknown. Here we show ELOVL fatty acid elongase 2 (Elovl2), a gene whose epigenetic alterations are most highly correlated with age prediction, contributes to aging by regulating lipid metabolism. Impaired Elovl2 function disturbs lipid synthesis with increased endoplasmic reticulum stress and mitochondrial dysfunction, leading to key accelerated aging phenotypes. Restoration of mitochondrial activity can rescue age-related macular degeneration (AMD) phenotypes induced by Elovl2 deficiency in human retinal pigmental epithelial (RPE) cells. We revealed an epigenetic–metabolism axis contributing to aging and potentially to antiaging therapy.

aging | epigenetic alteration | lipid metabolism | ER stress | mitochondrial dysfunction

Aging is an inevitable life process characterized by increasing vulnerability to disease, loss of molecular fidelity, and progressive decline in tissue and organ function (1). Epigenetic alterations play a key role in aging by integrating environmental signals to regulate gene expression and downstream cellular processes (2–6). The integral relationship between aging and DNA methylation levels was not clearly described until recently (7–10), Several hundred CpG sites with methylation levels correlating to biological age were precisely mapped (6, 11). Studies by several groups established epigenetic DNA methylation signatures (12) that can serve as an accurate biological age "clock" in many different tissue-types (12, 13) [see recent review by Bell et al. (14)], some of which were found within metabolism-associated genes which indicates an intimate association between epigenetic alterations and metabolism in aging (5).

Elovl2, a gene which functions as a master control of polyunsaturated fatty acid (PUFA) synthesis and is strongly associated with diabetes, shows the most relevance to aging (4, 11, 15, 16). The methylation status of Elovl2 explains 70% of the "aging epigenetic clock" (15). Several CG markers, including Elovl2, predict aging in various tissues (15, 17) and are referred to as universal bioage markers (15, 17), whereas the remaining markers are usually tissue specific and carry less weight in aging prediction. Functionally, Elovl2 plays an irreplaceable role in the synthesis of PUFAs, which are critical for a range of biological processes. It has been reported that the concentration of PUFAs in the body correlates negatively with age in human, including both their side chains and byproducts (18, 19). Although the role of Elovl2 in the synthesis of PUFAs has been well documented in previous studies, the effect of Elovl2 deficiency on aging or the downstream mechanism underlying how age-related Elovl2 methylation contributes to aging remains unknown.

We reasoned that decrease of Elovl2 expression contributed to aging by disrupting the balance of lipid metabolism in the endoplasmic reticulum (ER) and mitochondria. On one hand, Elvol2 is localized in the ER, where PUFAs are elongated. On the other hand, mitochondria is the main site of lipid degradation where fatty acid oxidation occurs. Both of them play important roles in lipid metabolism and aging. Here, we show that lack of Elovl2 leads to a decline in PUFA synthesis and the accumulation of short fatty acids including PUFA precursors in ER, altering mitochondrial energy metabolism and resulting in chronic ER stress and mitochondria dysfunction. These changes resulted in aging phenotypes, including stem cell exhaustion, cognitive decline, retinal degeneration, and glucose intolerance.

Results

Increased Methylation with Concomitant Decreased Gene Expression of Elovl2 Correlates with Biological Aging. We and others have reported a group of genes in human and mice for which methylation

Significance

ELOVL fatty acid elongase 2 (Elovl2), a gene whose methylation values are most highly correlated with age prediction, contributes to aging by regulating lipid metabolism. Impaired Elovl2 function disturbs lipid synthesis with increased endoplasmic reticulum stress and mitochondrial dysfunction, leading to key accelerated aging phenotypes. Restoration of mitochondrial activity can rescue age-related macular degeneration (AMD) phenotypes induced by Elovl2 deficiency in human retinal pigmental epithelial (RPE) cells. Our study reveals a key role of epigenetic–metabolism axis contributing to aging and provides an avenue for antiaging therapy.

Author contributions: X.L., J.W., J.-K.Z., W.L., Q.Z., and K.Z. designed research; X.L., J.W., L.W., G.F., G.L., M.Y., Y.L., C.L., X.Y., G.Z., Z.L., L.Z., H.O., Q.Q., G.W., C.Z., O.L., J.X., J.-K.Z., W.L., Q.Z., and K.Z. performed research; X.L., J.W., L.W., G.F., G.L., L.Z., J.-K.Z., W.L. Q.Z., and K.Z. analyzed data; X.L., J.W., G.F., J.-K.Z., Q.Z., and K.Z. wrote the paper; and Q.Z. and K.Z. supervised research.

Reviewers: S.B., University College London Cancer Institute; H.D., Peking University; and A.E.T., Chinese Academy of Sciences–Max Planck Gesellschaft Partner Institute for Computational Biology.

The authors declare no competing interest.

Data deposition: The sequencing data reported in this paper have been deposited in Genome Sequence Archive of Beijing Institute of Genomics, Chinese Academy of Sciences (http://gsa.big.ac.cn/). The accession numbers for mouse and human data are CRA002140 and CRA002141.

[1]X.L., J.W., L.W., G.F., and G.L. contributed equally to this work.

[2]To whom correspondence may be addressed. Email: kang.zhang@gmail.com, qzhou@ioz.ac.cn, liwei@ioz.ac.cn, or jkzhu@sibs.ac.cn.

This article contains supporting information online at https://www.pnas.org/lookup/suppl/doi:10.1073/pnas.1919403117/-/DCSupplemental.

First published February 6, 2020.

level corelated with aging; consequently, these genes can serve as predictors for biological age (6, 11). Consistent with previous reports (4, 11, 15), we observed that lipid storage, fatty acid metabolism, and lipogenesis-associated genes were revealed in Gene Ontology (GO) term analysis of top relevant predictor genes. Among the top predictor genes, Elovl2 loci show the most significant relevance to biological age (Fig. 1*A* and *SI Appendix*, Fig. S1*A*). A similar age-related methylation pattern was confirmed in both human in vitro cell models and mouse in vivo models. By using a human fibroblast cell model, a dramatic increase of methylation on Elovl2 accompanied with down-regulating Elovl2 expression level was detected in aged human fibroblasts (38 passages) (Fig. 1*B*). Next, we examined CpG islands within the Elovl2 gene in different mouse tissue at different ages: CpG island (CGI)-I1 in the first intron, and CGI-E3, -E4, and -E8 in the third, fourth, and eighth exons (*SI Appendix*, Fig. S1*B*). We found that the methylation of CGI-I1, -E3, -E4, and -E8 in brain and liver significantly increased with aging in 129/sv strains (Fig. 1*C* and *SI Appendix*, Fig. S1 *C* and *D*). Besides, qPCR analysis showed that the expression level of Elovl2 decreased with aging in 129 mice (*SI Appendix*, Fig. S1*E*). A consistent result was observed in the ICR mouse strain (*SI Appendix*, Fig. S1 *C–E*). These results indicated that Elovl2 showed a conserved pattern of increased methylation and reduced expression in both the human fibroblast cell model and the mouse model.

DNA Methylation of Elovl2 Is Mediated during Cellular Senescence and the DNA Damage Repair Process. Next, we investigated how environmental factors during the aging process affect DNA methylation of Elovl2. It has been argued that DNA damage is one of the most important drivers of aging (3, 20, 21). A previous report showed that chromodomain helicase DNA-binding protein 4 (CHD4), a key component of the nucleosome remodeling and histone deacetylation (NuRD) complex plays a central role in DNA damage repair-mediated gene silencing in cancer cells (22). Therefore, we hypothesized that age-related DNA methylation could also be mediated by DNA damage and its repair process. We used hydrogen peroxide (H_2O_2)-treated human fibroblasts as an aging model. After H_2O_2 treatment (100 μM 24 h), human fibroblast cells showed a significant up-regulation of senescent marker genes. This phenotype is consistent with the expression patterns in high-passage number (30 to 40 passages) cells (Fig. 1 *D* and *E* and *SI Appendix*, Fig. S1 *F* and *G*). In addition, the increased methylation of Elovl2 was observed in H_2O_2-treated cells (Fig. 1*F*), indicating that DNA methylation occurred in both H_2O_2-treated cells and high-passage number cells (Fig. 1*B*). Next, we examined whether CHD4 could interact with DNA methyltransferases (DNMTs) and chromatin suppression modifiers to mediate abnormal DNA methylation in the H_2O_2-treated fibroblast cells. Coimmunoprecipitation assays showed that CHD4 interacted significantly with DNMTs after H_2O_2 treatment (Fig. 1*G*). Western blotting further showed that the binding of DNMTs to chromatins was promoted by H_2O_2 treatment (Fig. 1*H*, tight chromatin, control), but was diminished by CHD4 knockdown (Fig. 1*H*, tight chromatin, iCHD4), indicating that the H_2O_2-induced accumulation of DNMTs to chromatins was CHD4 dependent. Other inhibitory histone modifiers, such as EZH2 and G9a, were also recruited by CHD4

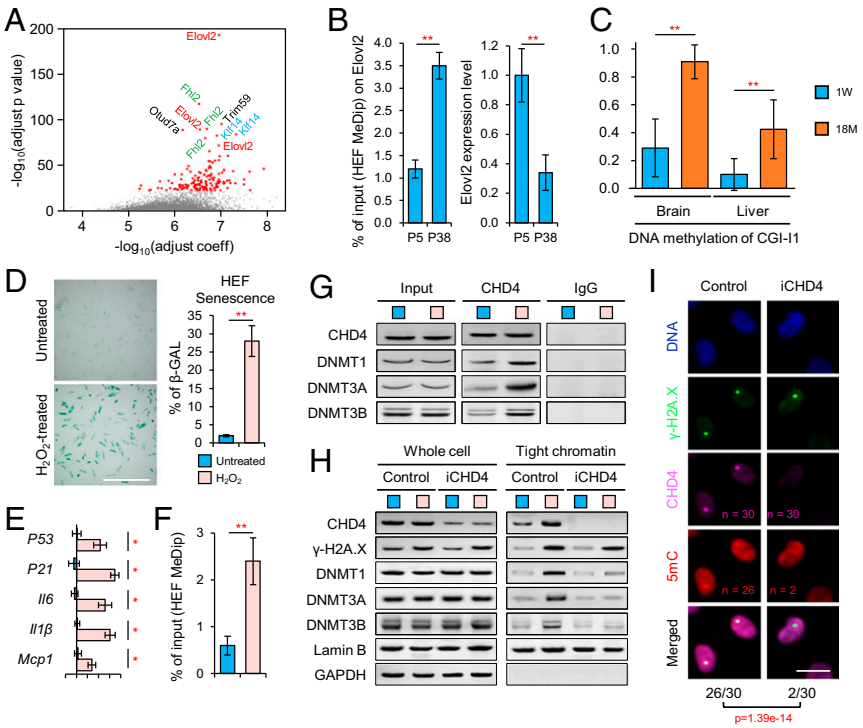

Fig. 1. Elovl2 is a metabolic gene that serves as a marker of aging. (*A*) Correlation between DNA methylation of genes and aging. The significant sites are marked. (*B*) MeDip-qPCR and qPCR of Elovl2 in human fibroblasts. Error bars, SEM. $^{**}P < 0.01$. Levels of significance were calculated with two-tailed Student's *t* test. (*C*) DNA methylation level on the CpG island in intron 1 (CGI-I1) of Elovl2 in the brain and liver of 129/sv mice. Error bars, SEM. $^{**}P < 0.01$. Levels of significance were calculated with two-tailed Student's *t* test. (*D*) β-Galactosidase (β-GAL) staining on young (p5) human fibroblasts with or without H_2O_2 treatment. (Scale bar, 100 μm.) $^{**}P < 0.01$. Levels of significance were calculated with two-tailed Student's *t* test. (*E*) qPCR showing the transcriptional changes of cellular senescence markers in normal and H_2O_2-treated human fibroblasts. Error bars, SEM. $^{*}P < 0.05$. Levels of significance were calculated with two-tailed Student's *t* test. (*F*) MeDip-qPCR of Elovl2 in H_2O_2-treated human fibroblasts. Error bars, SEM. $^{**}P < 0.01$. Levels of significance were calculated with two-tailed Student's *t* test. (*G*) Coimmunoprecipitation on human fibroblasts with or without H_2O_2 treatment. (*H*) Western blotting showing that the H_2O_2-induced accumulation of DNMTs to the chromatins was CHD4 dependent. (*I*) The recruitment of CHD4 and 5-mC on DNA damage sites of cells irradiated with a 450-nm laser. (Scale bar, 5 μm.) For each group, 30 cells were treated.

(*SI Appendix*, Fig. S1*H*). Furthermore, we were able to detect endogenous CHD4, γH2a.X, and increased 5-methylcytosine (5-mC) signals at the damage sites 60 min postlaser-induced DNA damages, which were dramatically reduced upon CHD4 knockdown (Fig. 1*I*), indicating that CHD4 plays a central role in DNA damage-mediated methylation during the repair process. Next, we compared the expression of Elovl2 in human fibroblasts before and after H_2O_2 treatment. The expression of Elovl2 was significantly decreased after H_2O_2 treatment in groups with individual DNMT knockdown, but not in the CHD4 knockdown group (*SI Appendix*, Fig. S1*I*), indicating that individual knockdown of single DNMT would not block H_2O_2-induced Elovl2 silencing. On the other hand, knockdown of CHD4 dramatically rescued the expression level of Elovl2 after H_2O_2 treatment, which indicated a central role in mediating DNA methylation and further down-regulating transcriptional activity of Elovl2. Overall, these results showed that age-related DNA methylation can be mediated by CHD4 upon DNA damage.

Deletion of Elovl2 Causes a Dramatic Accelerated Aging Phenotype in Mice. Previous studies on loss of Elovl2 function were mainly restricted to mouse development and lipid metabolism (19, 23), yet age-related phenotypes have not been studied. To examine the function of Elovl2 in aging, we generated Elovl2 knockout mice with CRISPR-Cas9 (*SI Appendix*, Fig. S2*A*). In total, we generated 40 Elovl2$^{+/-}$ and 84 Elovl2$^{-/-}$ founder mice. In the Elovl2$^{-/-}$ mice, 32 mice had a 59-bp deletion in the third exon that created a stop codon. Western blotting showed that Elovl2 was completely depleted (*SI Appendix*, Fig. S2*B*). Our experiments were performed on these 59-bp deletion mice because both Elovl2$^{+/-}$ and Elovl2$^{-/-}$ mice were infertile, irrespective of gender or strain; this was not consistent with previous reports (19). This may be caused by different knockout conditions and diet. Stringent non-PUFA milk and ingredient-defined non-PUFA diet were used for the pups or adult mice to prevent the consumption of PUFAs from the food intake. We then examined key aging parameters after 8 mo of growth. Elovl2$^{-/-}$ young mice ($^{-/-}$Y) displayed a series of aging-accelerated phenotypes, including hair loss (Fig. 2*A*) and reductions in bone density (Fig. 2*B* and *SI Appendix*, Fig. S2*C*), endurance (*SI Appendix*, Fig. S2*D*), and muscle strength (*SI Appendix*, Fig. S2*E*). Besides, the open-field behavior test showed that $^{-/-}$Y mice exhibited reduced exploratory behavior and increased anxiety that were similar to the behavior of wild-type old (WT-O, 20 mo old) mice (Fig. 2*C*). Furthermore, the Morris water maze test suggested a significant decay in learning and memorizing ability in $^{-/-}$Y mice (*SI Appendix*, Fig. S2*F*). Moreover, aging-related histopathological phenotypes were detected in $^{-/-}$Y and WT-O mice (Fig. 2*D* and *SI Appendix*, Fig. S2 *G* and *H*). These results demonstrate that lack of Elovl2 in mice leads to a remarkable acceleration of aging from multiple aspects.

Lack of Elovl2 Disturbs Lipid and Energetic Metabolism. Next, we investigated whether Elovl2 deficiency accelerated aging through impaired metabolism. Considering that Elovl2 plays a critical role in lipid metabolism by functioning as an elongase for long-chain fatty acids from 20: C to 28: C (19) (*SI Appendix*, Fig. S3*A*), we performed lipidomic analysis. There was a dramatic accumulation of fatty acids containing fewer than 20 carbons and depletion of PUFAs with carbon chains longer than 22: C, such as docosahexaenoic acid (DHA), in liver, brain, and plasma of WT-O and $^{-/-}$Y mice (Fig. 2*E* and *SI Appendix*, Fig. S3*B*). Using Oil Red O (ORO) staining, we observed substantial accumulation of fatty acids in hepatocytes in both WT-O and $^{-/-}$Y mice (Fig. 2*F*). Furthermore, a steatohepatitis phenotype was detected by ultrasonography in WT-O and $^{-/-}$Y mice (Fig. 2*G*). These changes could cause hepatic steatosis followed by lipotoxicity (24) and insulin resistance (25, 26). Then we performed a glucose tolerance test (GTT) and an insulin tolerance test (ITT). We observed dramatic glucose tolerance and insulin resistance phenotypes in the $^{-/-}$Y mice (Fig. 2*H* and *SI Appendix*, Fig. S3*C*). This result was consistent with a previous study which reported that the transcriptional activity of Elovl2 had an intimate connection with insulin secretion (16). Collectively, these results were indicative of severe metabolic dysfunction in Elovl2-deficient mice.

A Diet Supplemented with PUFAs Can Partially Rescue the Aging Phenotype in Elovl2 Knockout Mice. Knowing that lack of Elovl2 diminished the synthesis of PUFAs, we next investigated whether the dietary supplementation of PUFAs could fully rescue the accelerated aging phenotype. In comparison to the control group, dietary supplementation with PUFAs (fish oil) slightly ameliorated fatty acid accumulation in the livers of $^{-/-}$Y mice and improved physiological glucose metabolic balance, but was insufficient for complete recovery (Fig. 2 *G* and *H* and *SI Appendix*, Fig. S3*C*). An open-field behavioral test showed that dietary supplementation with PUFAs led to slight improvement of aging phenotypes (*SI Appendix*, Fig. S3*D*). Furthermore, the addition of PUFAs did not relieve aging-related histopathological phenotypes (*SI Appendix*, Fig. S3*E*). These results indicated that the contribution of lack of Elovl2 to aging did not occur solely through a deficit of nutrient PUFAs.

Lack of Elovl2 Leads to Chronic Inflammation and Adult Stem Cell Exhaustion in Mice. Adult stem cells are essential for the maintenance of tissue function and homeostasis. Metabolism plays a key role in maintaining an adult stem cell pool (27). Recently, Oishi et al. reported that lipid metabolism, particularly PUFA synthesis, plays a critical role in the immune response (28). PUFAs such as DHA and eicosapentaenoic acid (EPA), as precursors of inflammation inhibitors, can regulate inflammation (29, 30). In consideration of that, we hypothesized that $^{-/-}$Y mice would have extensive and serious chronic inflammation.

Indeed, the analysis of blood samples showed a significant increase in the levels of inflammatory factors in both $^{-/-}$Y and WT-O mice (Fig. 3*A* and *SI Appendix*, Fig. S4*A*). We also examined the status of inflammation in the liver and found that levels of MCP1 and TNF-α were dramatically increased in WT-O and $^{-/-}$Y mice (Fig. 3*B*). It is well known that chronic inflammation leads to tissue fibrosis and the exhaustion of endogenous stem/progenitor cell reservoirs (29, 30). In line with these expectations, we observed an increase of fibrosis in the liver (Fig. 3*C*). Furthermore, we detected a significant loss of the stem cell population in hair follicles (CK15) and in the intestine (LGR5) (Fig. 3*D*).

Increased terminal deoxynucleotidyl transferase dUTP nick end labeling (TUNEL) staining in the retina, particularly in the retinal pigmental epithelial (RPE) layer (Fig. 3*E*), along with a reduction in the thickness of the outer nuclear layer (ONL) (Fig. 3*F*), indicated an increased level of senescent signals. We also observed a decline in the visual function of photoreceptors in the retina of $^{-/-}$Y and WT-O mice (Fig. 3*G* and *SI Appendix*, Fig. S4*B*), coincident with the appearance of drusen (Fig. 3*E* and *SI Appendix*, Fig. S4*C*). Next, we examined the cerebral cortex and hippocampus structure by magnetic resonance imaging (MRI), which revealed a dramatic abnormity in $^{-/-}$Y and WT-O mice (*SI Appendix*, Fig. S4*D*). RNA-Seq analysis also showed a remarkably abnormal expression profile and impaired functional gene expression in the brains of $^{-/-}$Y mice (*SI Appendix*, Fig. S4 *E* and *F*). These results indicated that failure to resolve endogenous or extrinsic inflammatory stimuli in tissues' lack of Elovl2 led to chronic inflammation, stem cell exhaustion, and a loss of tissue function, which in turn resulted in aging phenotypes.

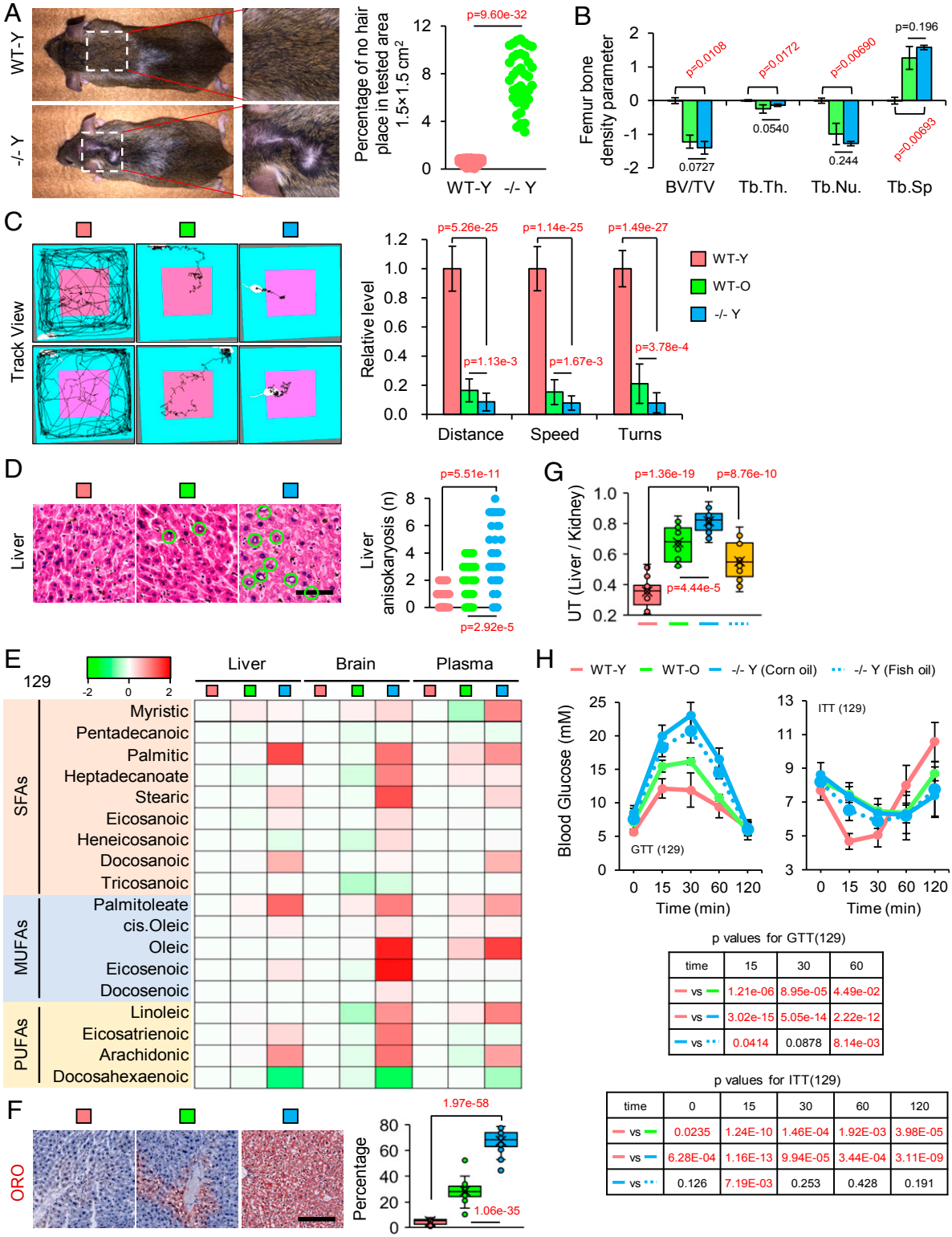

p values for GTT(129)

time	15	30	60
vs	1.21e-06	8.95e-05	4.49e-02
vs	3.02e-15	5.05e-14	2.22e-12
vs	0.0414	0.0878	8.14e-03

p values for ITT(129)

time	0	15	30	60	120
vs	0.0235	1.24E-10	1.46E-04	1.92E-03	3.98E-05
vs	6.28E-04	1.16E-13	9.94E-05	3.44E-04	3.11E-09
vs	0.126	7.19E-03	0.253	0.428	0.191

Fig. 2. Deletion of Elovl2 caused severely accelerated aging phenotypes and metabolic dysfunction in mice. (*A*) Hair loss in young (8 mo) Elovl2 knockout ($^{-/-}$ Y) but not wild type (WT-Y) 129/sv mice. (*B*) Microcomputed tomography (micro-CT) showing bone volume/total volume (BV/TV) and trabecular thickness (Tb.Th.) in the femur of mice. Error bars, SEM. Levels of significance were calculated with two-tailed Student's *t* test. Tb.Nu., trabecular number; Tb.Sp, trabecular spacing. (*C*) Open-field test results in different groups of 129/sv mice. Error bars, SEM. Levels of significance were calculated with two-tailed Student's *t* test. (*D*) Hematoxylin and eosin staining and pathological section analysis of liver tissue. Green cycles show the abnormal structures. (Scale bar, 100 μm.) Levels of significance were calculated with two-tailed Student's *t* test. (*E*) Heatmap of fatty acid species in the liver, brain, and plasma of 129/sv mice. (*F*) ORO staining of liver. Error bars, SEM. (Scale bar, 100 μm.) Levels of significance were calculated with two-tailed Student's *t* test. (*G*) Ultrasound test results. Error bars, SEM. Levels of significance were calculated with two-tailed Student's *t* test. (*H*) GTT and ITT results. Error bars, SEM. Levels of significance were calculated with two-tailed Student's *t* test.

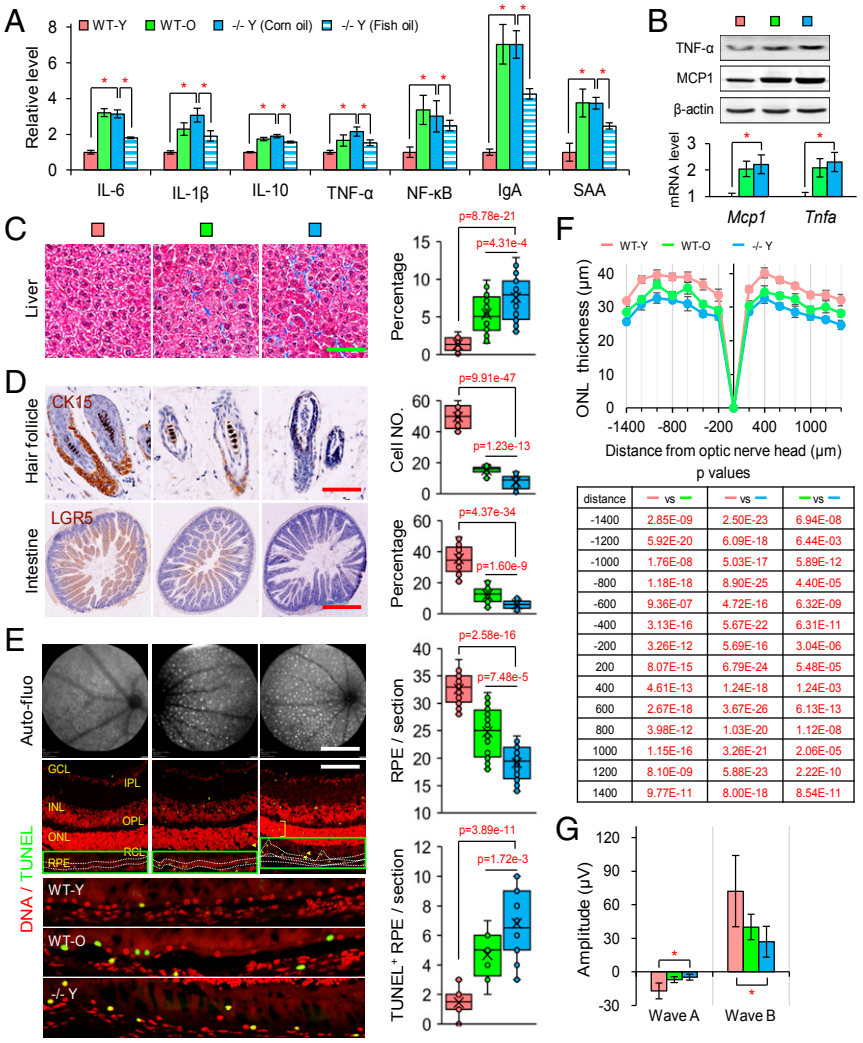

distance	vs	vs	vs
-1400	2.85E-09	2.50E-23	6.94E-08
-1200	5.92E-20	6.09E-18	6.44E-03
-1000	1.76E-08	5.03E-17	5.89E-12
-800	1.18E-18	8.90E-25	4.40E-05
-600	9.36E-07	4.72E-16	6.32E-09
-400	3.13E-16	5.67E-22	6.31E-11
-200	3.26E-12	5.69E-16	3.04E-06
200	8.07E-15	6.79E-24	5.48E-05
400	4.61E-13	1.24E-18	1.24E-03
600	2.67E-18	3.67E-26	6.13E-13
800	3.98E-12	1.03E-20	1.12E-08
1000	1.15E-16	3.26E-21	2.06E-05
1200	8.10E-09	5.88E-23	2.22E-10
1400	9.77E-11	8.00E-18	8.54E-11

Fig. 3. Depletion of Elovl2 led to chronic inflammation, cellular senescence, and adult stem cell exhaustion. (*A*) Inflammatory factor levels in blood. Error bars, SEM. *$P < 0.05$. Levels of significance were calculated with two-tailed Student's *t* test. (*B*) Western blotting and qPCR of TNF-α and MCP-1. Error bars, SEM and *$P <$ 0.05. Levels of significance were calculated with two-tailed Student's *t* test. (*C*) Masson's trichrome staining on liver. Error bars, SEM. (Scale bar, 100 μm.) Levels of significance were calculated with two-tailed Student's *t* test. (*D*) Hair follicles and intestines stained with the epithelial progenitor cell markers. (Scale bar, 100 μm.) Error bars, SEM. Levels of significance were calculated with two-tailed Student's *t* test. (*E*) Autofluorescence images of the fundus drusen; propidium staining (red) showing different layers of retina, including ganglion cell layer (GCL), inner plexiform layer (OPL), outer nuclear layer (ONL), layers of rods and cones (RCL), and retina pigment epithelium (RPE); TUNEL staining (green) showed apoptosis. Error bars, SEM. (Scale bar, 800 μm for autofluorescence images and 100 μm for slices.) Levels of significance were calculated with two-tailed Student's *t* test. (*F*) The thickness of the ONL layer. Error bars, SEM. Levels of significance were calculated with two-tailed Student's *t* test. (*G*) Visual function analysis. Error bars, SEM. *$P < 0.05$. Levels of significance were calculated with two-tailed Student's *t* test.

RNA-Seq Analysis Indicates Various Metabolic and Aging-Related Pathways Were Impaired by Elovl2 Depletion. To identify the molecular mechanism responsible for loss of Elovl2 in aging, we performed RNA-Seq on liver and brain samples from wild type-young (WT-Y) and $^{-/-}$ Y mice. Compared to the up-regulation of genes in WT-O mice reported in previous studies (31), these genes were also enriched in our $^{-/-}$ Y mice (Fig. 4*A*); the down-regulated genes also showed a consistent pattern (Fig. 4*A*). Interestingly, we found that $^{-/-}$ Y mice had a similar expression profile to those on a high-fat diet (HFD) (32), which verified that Elovl2 ablation resulted in fatty acid accumulation (*SI Appendix*, Fig. S5*A*). We identified 1,867 differentially expressed genes (twofold change and *P* value <0.05) in the liver of $^{-/-}$ Y mice compared to that of WT-Y mice, with 1,084 genes up-regulated and 783 genes down-regulated. GO enrichment analyses showed that fatty acid/lipid metabolism, cellular responses to insulin stimulus, mitochondrial function, and uncoupled protein response were misregulated (Fig. 4*B*). Notably, we found that the ER stress-associated genes were up-regulated (Fig. 4*C* and *SI Appendix*, Fig. S5*B*), which was consistent with a previous study which reported that lipotoxicity leads to ER stress (25, 26). It is well known that both lipotoxicity and ER stress can impair mitochondrial function. Indeed, we found that mitochondrial function-associated genes, such as those involved in the fatty acid β-oxidation process and insulin receptor signaling pathway, were down-regulated, while mitochondrial uncoupled protein response (UPR^{mt})- and glycolysis-associated genes were up-regulated (Fig. 4*C*). Consistent with RNA-Seq data, qPCR also showed the same expression patterns (*SI Appendix*, Fig. S5*C*).

Impaired Lipid Metabolism Causes a Stress Response in the ER and Mitochondrial Dysfunction. Mitochondria participate in the aging process in multiple ways, such as energy production, the generation of reactive oxygen species (ROS), and UPR^{mt}. Also, mitochondria can contribute to changes in the cellular senescence state (33–36). Therefore, based on our RNA-Seq data analysis and clues from

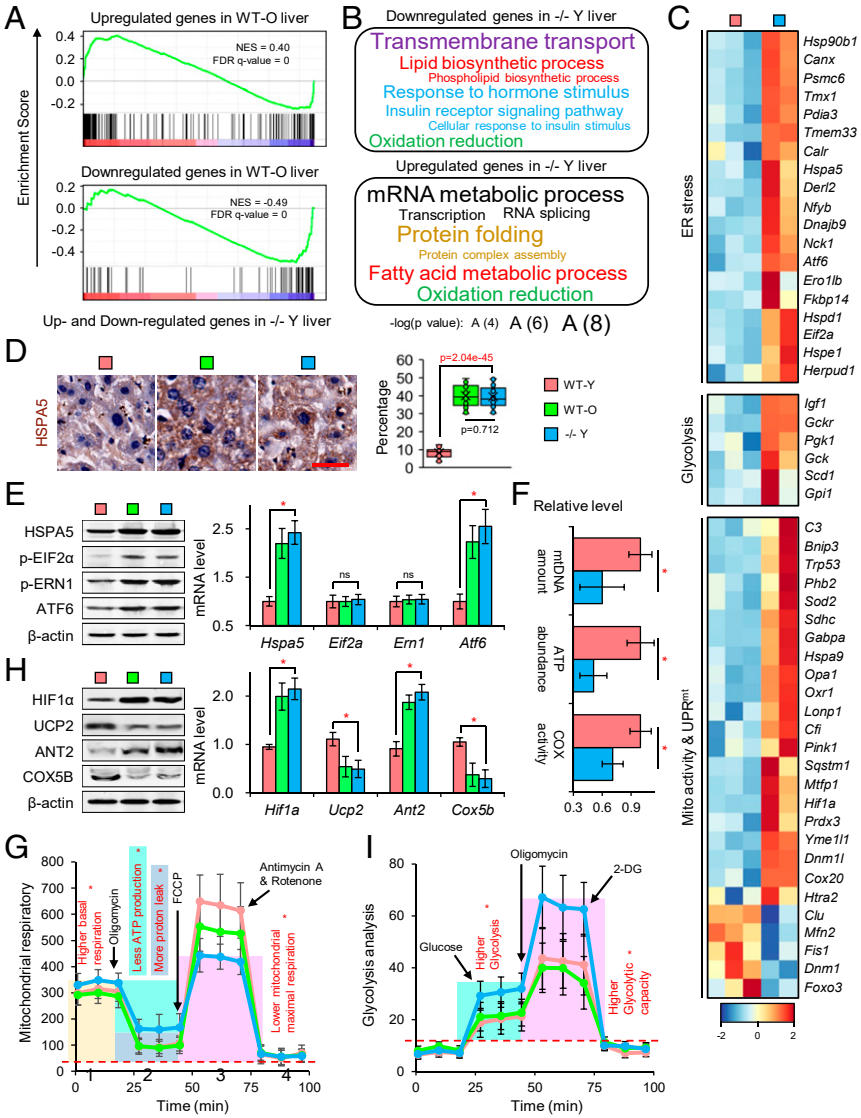

Fig. 4. Elovl2 deficiency led to endoplasmic reticulum stress and mitochondrial dysfunction. (*A*) Enriched gene sets of differentially expressed genes in $^{-/-}$ Y samples. The horizontal axis represents the differentially expressed genes in $^{-/-}$ Y compared to WT-O samples which were ranked as either up- or down-regulated in $^{-/-}$ Y and marked in red and blue, respectively. The normalized enrichment score (NES) and false discovery rate (FDR) are marked. (*B*) The Gene Ontology terms enriched in up- or down-regulated genes in $^{-/-}$ Y. (*C*) Expression pattern of genes in aging-related pathways. (*D*) HSPA5 staining in liver. Error bars, SEM. Levels of significance were calculated with two-tailed Student's *t* test. (*E*) Western blotting and qPCR for the markers of ER stress. Error bars, SEM. $*P < 0.05$; ns, $P > 0.5$. Levels of significance were calculated with two-tailed Student's *t* test. (*F*) Mitochondrial function analysis. Error bars, SEM. $*P < 0.05$. Levels of significance were calculated with two-tailed Student's *t* test. (*G*) The Seahorse XF Mitochondrion Stress Test. Error bars, SEM. $*P < 0.05$. Levels of significance were calculated with two-tailed Student's *t* test. (*H*) Western blotting and RT-qPCR of HIF1α, ANT2, UCP2, and COX5b. Error bars, SEM. $*P < 0.05$. Levels of significance were calculated with two-tailed Student's *t* test. (*I*) The Seahorse XF Glycolysis Test. Error bars, SEM. $*P < 0.05$. Levels of significance were calculated with two-tailed Student's *t* test.

previous reports, we hypothesized that lack of Elovl2 promotes aging-inducing ER stress and mitochondrial dysfunction.

To verify our hypothesis, we measured ER stress levels and mitochondrial function in liver tissues. ER stress markers, such as HSPA5, phosphorylated EIF2α (p-EIF2α), p-ERN1, and ATF6, were up-regulated in WT-O and $^{-/-}$ Y mice (Fig. 4 *D* and *E*). Furthermore, mtDNA content, ATP abundance, and COX activity were dramatically reduced in WT-O and $^{-/-}$ Y mice. WT-Y mice showed a relatively high level of mitochondrial activity (Fig. 4*F*).

We then used the Agilent Seahorse XF Cell Mito Stress Test to investigate key parameters of mitochondrial function by directly measuring the oxygen consumption rate (OCR) of primary hepatocytes from WT-O and $^{-/-}$ Y mice. For basal respiration, we found that the OCR was significantly increased in $^{-/-}$ Y mice (Fig. 4*G*, 1), which was not diminished by oligomycin treatment, suggesting an increased incidence of uncoupled respiration (Fig. 4*G*, 2). Consistently, we found up-regulated expression of HIF1α and ANT2, while the expression of UCP2 was down-regulated (Fig. 4*H*), indicating there is hypoxia-mediated mitochondrial dysfunction in $^{-/-}$ Y mice which may also result from superfluous fatty acids (37, 38).

Predictably, after the addition of carbonyl cyanide-4-(trifluoromethoxy) phenylhydrazone (FCCP), there was a lower level of mitochondrial maximal respiration in $^{-/-}$ Y mice (Fig. 4*G*, 3), consistent with a lower level of COX5b and reflecting reduced activity of the oxidation respiratory chain (Fig. 4*H*). In addition, we found that $^{-/-}$ Y mice showed increased glycolytic activity (Fig. 4*I*). A switch of metabolism from oxidative phosphorylation to glycolysis, known as the Warburg effect, was observed in both cancerous and senescent cells. It was also identified in our RNA-Seq data (Fig. 4*C*).

One of the consequences of chronic ER stress and mitochondrial dysfunction is oxidative damage at the cellular level. Using varied means of detection, we found that oxidative damage developed in both mitochondria (*SI Appendix*, Fig. S5*D*, MitoSOX for mitochondrial superoxide) and nuclei (*SI Appendix*, Fig. S5*D*, γ-H2aX for DNA oxidative damage), affecting proteins (*SI Appendix*, Fig. S5*E*, AOPP), lipids (*SI Appendix*, Fig. S5*E*, MDA), and RNA (*SI Appendix*, Fig. S5*E*, 8-OHG). As expected, antioxidative enzymes were overactivated (*SI Appendix*, Fig. S5*E*, GSH-PX, CAT, T-SOD, and TAC). Notably, upon such severe oxidative damage, higher cellular senescent markers were detected in $^{-/-}$ Y and WT-O mice (*SI Appendix*, Fig. S5*F*).

In summary, Elovl2 absence could lead to short-chain fatty acid accumulation, ER stress, and mitochondrial dysfunction at cellular level.

Elovl2 Deficiency in Human RPE Cells Induces an Age-Related Macular Degeneration Phenotype. After our results showed that the depletion of Elovl2 leads to an age-related macular degeneration (AMD) phenotype in mice, we next investigated whether Elovl2

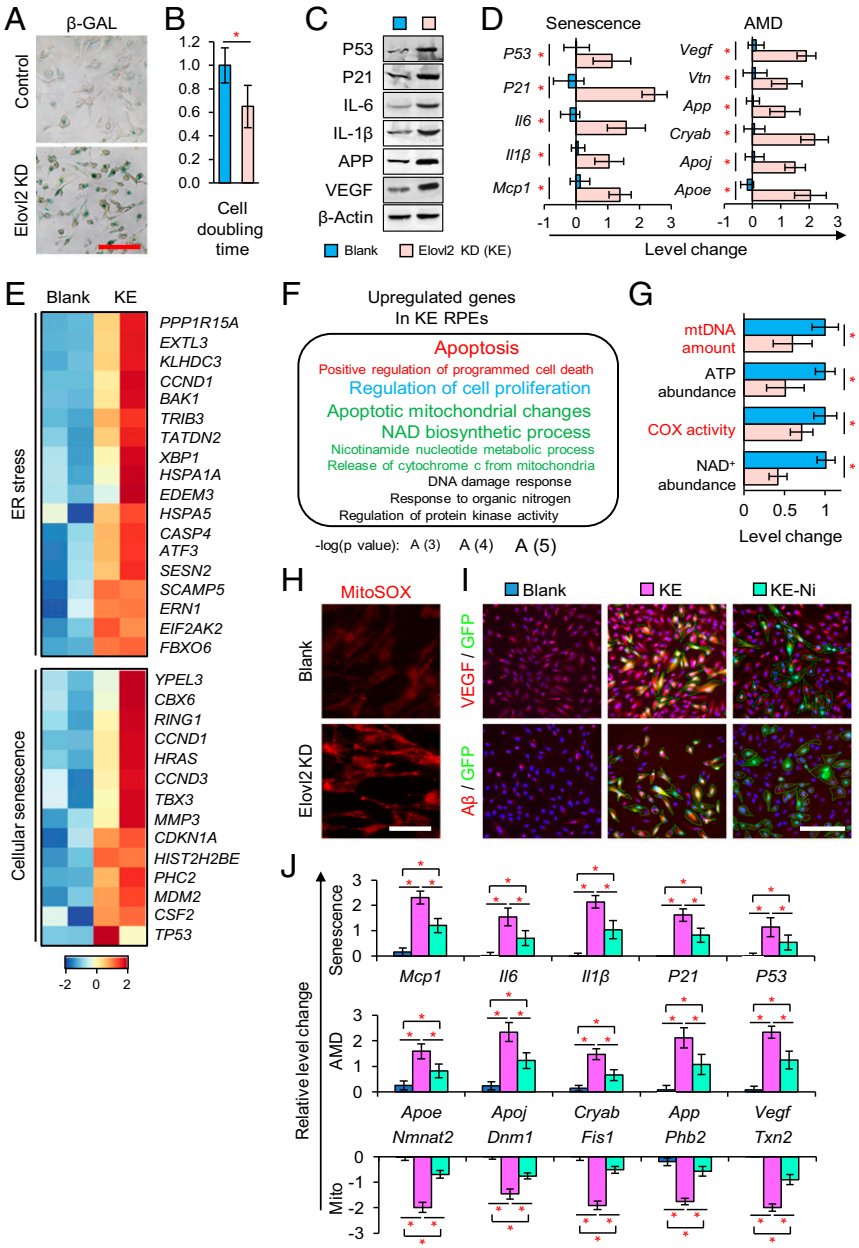

Fig. 5. AMD phenotype induced by the depletion of Elovl2 in human RPE cells. (*A*) β-Galactosidase staining on human RPE cells with no treatment (blank, blue) or Elovl2 knockdown (KE, purple). (Scale bar, 100 μm.) (*B*) Cell doubling time analysis. Error bars, SEM. *$P < 0.05$. Levels of significance were calculated with two-tailed Student's *t* test. (*C* and *D*) Western blotting (*C*) and qPCR (*D*) of senescence and AMD marker in blank and KE cells. *$P < 0.05$. Levels of significance were calculated with two-tailed Student's *t* test. (*E*) The expression pattern of genes in ER stress- and cellular senescence-related pathways. (*F*) The Gene Ontology terms enriched in up-regulated genes in KE RPE cells. (*G*) Mitochondrial function analysis. Error bars, SEM. *$P < 0.05$. Levels of significance were calculated with two-tailed Student's *t* test. (*H*) mitoSOX staining results. (Scale bar, 100 μm.) (*I*) Immunofluorescence of blank and KE RPE cells treated with nicotinamide riboside (Ni) with VEGF and Aβ antibodies. (Scale bar, 100 μm.) (*J*) qPCR analysis of cells undergoing various treatments for cellular senescence, AMD, and mitochondrial function associated genes. Error bars, SEM. *$P < 0.05$. Levels of significance were calculated with two-tailed Student's *t* test.

ablation could result in an AMD phenotype in human cells. We developed Elovl2 knockdown RPE cell lines (KE) via the lentivirus delivery of shRNAs to human primary RPE cells (generated from healthy donors) (*SI Appendix*, Fig. S6 *A* and *B*). As expected, the knockdown of Elovl2 resulted in cellular senescence (Fig. 5*A*) and impaired proliferation (Fig. 5*B*) (33). We also detected the up-regulation of the senescence-associated secretory phenotype (SASP) markers, including P53, P21, IL-1b, IL-6, and MCP1 (35) in KE cells (Fig. 5*C*). Numerous senescence and AMD markers were found to be increased at both the RNA and protein levels in KE cells (Fig. 5*D*). These results indicated that an AMD model, with an increased SASP phenotype, can be generated by the deficiency of Elovl2 in human RPE cells.

As mentioned above, lack of Elovl2 led to fatty acid accumulation, which triggered chronic ER stress and mitochondrial dysfunction. Thus, we hypothesized that these impairments also occur in the Elovl2 deficiency-induced human AMD model. Indeed, from RNA-Seq analysis, we found a dramatic increase in chronic ER stress and cellular senescence in KE cells (Fig. 5*E* and *SI Appendix*, Fig. S6*C*). Moreover, GO term analysis showed mitochondrial dysfunction in KE cells; genes associated with mitochondrial function, such as those controlling the nicotinamide adenine dinucleotide (NAD) biosynthetic process and apoptotic mitochondrial changes, were dysregulated (Fig. 5*F* and *SI Appendix*, Fig. S6*D*). Consistent with this, we found that the KE cells showed a reduced amount of mitochondria and a loss of mitochondrial function (Fig. 5*G*). Furthermore, we detected the accumulation of oxidative damage in the mitochondria (Fig. 5*H*), which reflected severe oxidative damage in KE cells. In both the mouse and human cell models, Elovl2 deficiency led to an increase in oxidative damage caused by chronic ER stress and mitochondrial dysfunction.

Mitochondrial abnormalities are an early driver of neuronal dysfunction. It has been reported that restoration of mitochondrial function by NAD^+ precursor nicotinamide (vitamin B3) was protective both prophylactically and as an intervention against glaucoma, a neurodegenerative diseases that cause vision loss, especially in the elderly (36). To further confirm whether restoration of mitochondria can rescue AMD phenotype in Elovl2 knockdown RPE cells, we treated the Elovl2 knockdown RPE cells with nicotinamide (Ni). Interestingly, treatment with Ni during the culturing of KE cells dramatically reversed the abnormal expression of cellular senescence genes and reduced mitochondrial dysfunction, thus causing a remarkable reduction of AMD markers (Fig. 5 *I* and *J*). Together, these results indicated that restoration of mitochondria function can ameliorate the AMD phenotype caused by Elovl2 depletion.

Discussion

Epigenetic alteration is one of the hallmarks of aging. The integral relationship between aging and DNA methylation levels was established in the late 1960s; however, it was only recently that correlation between DNA methylation in several hundred CpG sites and biological age were precisely established (6, 11). We and others have shown that the DNA methylation of specific gene loci can be used as an accurate biomarker of biological aging in human and mice (4, 11, 15, 16). The functional consequences of methylation on these CpG sites have become attractive issues in many discussions and speculations. In our previous report, we identified a series of aging markers; some of these marker genes are involved in lipid metabolism. Intriguingly, Elovl2, a gene which functions as a master control of lipid metabolism and is strongly associated with diabetes, shows the most relevance to aging (4, 11, 15, 16). Slieker et al. (39) claimed that ELOVL2 is a unique tissue-independent age-associated DNA methylation marker; however, a subsequent report showed that ELOVL2 is not a unique universal aging marker and that there are many more CpG sites/genes that are consistently altered with age across many different cell/tissue types. Some of them map to genes in Wnt and glutamate receptor signaling pathways and are altered with age across at least 10 different cell/tissue types (17). This intriguing observation also indicates a potentially important role of the Wnt pathway in aging, since the Wnt pathway intimately contributes to maintaining the adult stem cell pool during aging. Further study needs to be done in this emerging field.

The mechanism of how aging-related methylation is mediated remains unclear. Cellular damage plays a key role in initiating epigenetic gene silencing (3, 20, 21). The transcription repressors can be immediately recruited to silence transcription on the site soon after DNA damage occurs (22). Chromatin silencing is required to ensure the damage repair process. Meanwhile, the subsequent abnormal DNA methylation was retained after this process. Here we showed that the NuRD complex plays a key role in the mediation of methylation on these age-related sites during cellular oxidative damage or following DNA double-/single-strand breaks. However, it still needs future study to learn the mechanism of random DNA damage-induced DNA methylation.

Elovl2, an important aging marker, plays a critical role in very long-chain fatty acid elongation. Previous studies show that Elovl2 is also associated with diabetes by genomewide association studies in mouse models (16), supporting the notion that Elovl2 is a crucial link between metabolism and aging. Here, we investigated whether Elovl2 played a functional role in aging first in a genetically modified mouse model. Although the life span of human and mouse is largely different (particularly the maximum life span differs dramatically), the shape of the theoretical lifespan curves, often considered representative of the health of the organism, is remarkably consistent across species (40). Several review papers have nicely shown the conserved phenotype and mechanism of aging shared in both human and mouse; some of these are even remarkably consistent across species, including yeast, worm, and flies. Indeed, López-Otín et al. have categorized these conserved features of aging into a set of nine "hallmarks of aging" (41), many of which span the evolutionary distance from yeast to human. The nine identified hallmarks of aging are as follows: genomic instability, mitochondrial dysfunction, deregulated nutrient sensing, loss of proteostasis, epigenetic alterations, cellular senescence, stem cell exhaustion, altered intracellular communication, and telomere attrition. In this study we used CRISPR-Cas9 to generate Elovl2 knockout mice. In contrast to previous reports, in our study we found a dramatic aging acceleration phenotype and many features of the nine hallmarks of aging in the Elovl2 knockout mice, suggesting its crucial role in the aging process.

Lipid synthesis is based on the normal function of ER, the location of Elovl2. Apart from lipid synthesis, the ER also performs important functions related to the synthesis, folding, and transport of proteins. It has previously been reported that the accumulation of free fatty acids in the ER would damage ER function, resulting in an increased incidence of unfolded or misfolded protein load and chronic ER stress. A reduction in PUFA synthesis upon Elovl2 ablation leads to a compensatory increase in fatty acid synthesis which can affect cellular metabolic homeostasis through the accumulation of fatty acid precursors for PUFAs in the ER and changes in mitochondrial energy metabolism. ER stress is also related to insulin resistance and mitochondrial dysfunction (*SI Appendix*, Fig. S7).

Mitochondria are the powerhouses of the cell and play a prominent role in producing energy through respiration and regulating cellular metabolism (34, 35). Elovl2 deficiency induced a switch in metabolism from the tricarboxylic acid (TCA) cycle to glycolysis, an effect which produces more ROS, causes oxidative stress in cells, tissues, and organs, and also act as a messenger for inflammatory responses. In addition, PUFAs are

essential in the resolution of inflammation. In this context, there were notable increases in physiological inflammation, cellular senescence, and adult stem cell exhaustion in a range of tissues in Elovl2 knockout mice (*SI Appendix*, Fig. S7). Next, we confirmed that this epigenetic–metabolism–aging axis also exists in humans. Increased levels of AMD markers were detected with similar accumulations of ER stress, mitochondrial dysfunction, and cellular senescence in human primary RPE cells. The restoration of mitochondrial activity by nicotinamide dramatically reduced the levels of AMD markers in Elovl2 knockdown human RPE cells.

Our result shows that epigenetic changes alter metabolism during aging and provide a better understanding of the molecular mechanisms underlying the epigenetic and metabolic aging process. Metabolic dysfunction is an effector of age-related epigenetic alterations. Meanwhile, metabolic dysfunction can also be a mediator that causes epigenetic changes reciprocally. The mechanism of how metabolism regulates age-related epigenetic alteration still needs to be further studied.

Materials and Methods

Detailed methods including experimental models, data source, cell culture, immunohistochemistry, molecular and biochemical analyses, functional assessments of Elovl2 knockdown cell culture and knockout mice, and statistical analysis are provided in *SI Appendix*. Sequencing and data analysis, DNA extraction, cell culture, colony formation assays, and tumor xenografts can be found in *SI Appendix*.

Data and Materials Availability. All data are available in the main text or *SI Appendix*. The sequencing data reported in this paper have been deposited in Genome Sequence Archive of Beijing Institute of Genomics, Chinese Academy of Sciences (http://gsa.big.ac.cn/). The accession numbers for mouse and human data are CRA002140 and CRA002141.

ACKNOWLEDGMENTS. We thank Qi Cheng and Junqiang Liang from Beijing Health OLight Technology Co. Ltd for their help with optical coherence tomography (OCT) and electroretinogram (ERG) services. We thank Chenghe Li, Wenqiang Gan, and Tiegang Li from the Institute of Materia Medica, Chinese Academy of Medical Sciences, and Peking Union Medical College for their help with the pathology section and MRI services. We thank Shiwen Li and Xili Zhu from the Institute of Zoology, Chinese Academy of Sciences, for their technical assistance. We thank Eppendorf, Leica, and Beckman for supplying the devices. This work was supported by grants from the Strategic Priority Research Program of the Chinese Academy of Sciences (XDA16030400 to Q.Z. and W.L.); National Natural Science Foundation of China (31621004 to Q.Z. and W.L., 31471395 to Q.Z., and 31701286 to G.F.); Guangzhou Regenerative Medicine and Health Guangdong Laboratory (to G.Z. and Z.L.); the Key Research Projects of the Frontier Science of the Chinese Academy of Sciences (QYZDY-SSW-SMC002 to Q.Z.); the Key Deployment Projects of the Chinese Academy of Sciences (ZDRW-ZS-2017-4 to W.L.); the National Basic Research Program of China (2014cB964801 to W.L.); the China Postdoctoral Science Foundation (2017M610990 and 2017T100107 to J.W.); the China National Postdoctoral Program for Innovative Talents (BX201700243 to L.W.); and the National Key Research and Development Program (2017YFA0103803 to Q.Z.).

1. C. López-Otín, L. Galluzzi, J. M. P. Freije, F. Madeo, G. Kroemer, Metabolic control of longevity. *Cell* **166**, 802–821 (2016).
2. L. N. Booth, A. Brunet, The aging epigenome. *Mol. Cell* **62**, 728–744 (2016).
3. B. A. Benayoun, E. A. Pollina, A. Brunet, Epigenetic regulation of ageing: Linking environmental inputs to genomic stability. *Nat. Rev. Mol. Cell Biol.* **16**, 593–610 (2015).
4. R. Zbieć-Piekarska *et al.*, Examination of DNA methylation status of the ELOVL2 marker may be useful for human age prediction in forensic science. *Forensic Sci. Int. Genet.* **14**, 161–167 (2015).
5. S. Han *et al.*, Mono-unsaturated fatty acids link H3K4me3 modifiers to C. elegans lifespan. *Nature* **544**, 185–190 (2017).
6. T. M. Stubbs *et al.*; BI Ageing Clock Team, Multi-tissue DNA methylation age predictor in mouse. *Genome Biol.* **18**, 68 (2017).
7. M. F. Fraga, M. Esteller, Epigenetics and aging: The targets and the marks. *Trends Genet.* **23**, 413–418 (2007).
8. M. F. Fraga *et al.*, Epigenetic differences arise during the lifetime of monozygotic twins. *Proc. Natl. Acad. Sci. U.S.A.* **102**, 10604–10609 (2005).
9. J. P. Issa, Age-related epigenetic changes and the immune system. *Clin. Immunol.* **109**, 103–108 (2003).
10. M. Toyota, M. Ohe-Toyota, N. Ahuja, J. P. J. Issa, Distinct genetic profiles in colorectal tumors with or without the CpG island methylator phenotype. *Proc. Natl. Acad. Sci. U.S.A.* **97**, 710–715 (2000).
11. G. Hannum *et al.*, Genome-wide methylation profiles reveal quantitative views of human aging rates. *Mol. Cell* **49**, 359–367 (2013).
12. A. E. Teschendorff *et al.*, Age-dependent DNA methylation of genes that are suppressed in stem cells is a hallmark of cancer. *Genome Res.* **20**, 440–446 (2010).
13. S. Horvath, DNA methylation age of human tissues and cell types. *Genome Biol.* **14**, R115 (2013). Erratum in: *Genome Biol.* **16**, 96 (2015).
14. C. G. Bell *et al.*, DNA methylation aging clocks: Challenges and recommendations. *Genome Biol.* **20**, 249 (2019).
15. R. C. Slieker, C. L. Relton, T. R. Gaunt, P. E. Slagboom, B. T. Heijmans, Age-related DNA methylation changes are tissue-specific with ELOVL2 promoter methylation as exception. *Epigenetics Chromatin* **11**, 25 (2018).
16. C. Cruciani-Guglielmacci *et al.*, Molecular phenotyping of multiple mouse strains under metabolic challenge uncovers a role for *Elovl2* in glucose-induced insulin secretion. *Mol. Metab.* **6**, 340–351 (2017).
17. T. Zhu, S. C. Zheng, D. S. Paul, S. Horvath, A. E. Teschendorff, Cell and tissue type independent age-associated DNA methylation changes are not rare but common. *Aging (Albany N.Y.)* **10**, 3541–3557 (2018).
18. A. M. Pauter *et al.*, Elovl2 ablation demonstrates that systemic DHA is endogenously produced and is essential for lipid homeostasis in mice. *J. Lipid Res.* **55**, 718–728 (2014).
19. D. Zadravec *et al.*, ELOVL2 controls the level of n-6 28:5 and 30:5 fatty acids in testis, a prerequisite for male fertility and sperm maturation in mice. *J. Lipid Res.* **52**, 245–255 (2011).
20. J. H. Chen, C. N. Hales, S. E. Ozanne, DNA damage, cellular senescence and organismal ageing: Causal or correlative? *Nucleic Acids Res.* **35**, 7417–7428 (2007).
21. L. Guarente, Linking DNA damage, NAD(+)/SIRT1, and aging. *Cell Metab.* **20**, 706–707 (2014).
22. L. Xia *et al.*, CHD4 has oncogenic functions in initiating and maintaining epigenetic suppression of multiple tumor suppressor genes. *Cancer Cell* **31**, 653–668.e7 (2017).
23. A. M. Pauter *et al.*, Both maternal and offspring Elovl2 genotypes determine systemic DHA levels in perinatal mice. *J. Lipid Res.* **58**, 111–123 (2017).
24. N. Alkhouri, L. J. Dixon, A. E. Feldstein, Lipotoxicity in nonalcoholic fatty liver disease: Not all lipids are created equal. *Expert Rev. Gastroenterol. Hepatol.* **3**, 445–451 (2009).
25. P. Ferré, F. Foufelle, Hepatic steatosis: A role for de novo lipogenesis and the transcription factor SREBP-1c. *Diabetes Obes. Metab.* **12** (suppl. 2), 83–92 (2010).
26. L. Salvadó, X. Palomer, E. Barroso, M. Vázquez-Carrera, Targeting endoplasmic reticulum stress in insulin resistance. *Trends Endocrinol. Metab.* **26**, 438–448 (2015).
27. M. Mohrin *et al.*, Stem cell aging. A mitochondrial UPR-mediated metabolic checkpoint regulates hematopoietic stem cell aging. *Science* **347**, 1374–1377 (2015).
28. Y. Oishi *et al.*, SREBP1 contributes to resolution of pro-inflammatory TLR4 signaling by reprogramming fatty acid metabolism. *Cell Metab.* **25**, 412–427 (2017).
29. C. D. Buckley, D. W. Gilroy, C. N. Serhan, Proresolving lipid mediators and mechanisms in the resolution of acute inflammation. *Immunity* **40**, 315–327 (2014).
30. C. N. Serhan, Pro-resolving lipid mediators are leads for resolution physiology. *Nature* **510**, 92–101 (2014).
31. R. R. White *et al.*, Comprehensive transcriptional landscape of aging mouse liver. *BMC Genomics* **16**, 899 (2015).
32. J. Y. Choi *et al.*, The metabolic response to a high-fat diet reveals obesity-prone and -resistant phenotypes in mice with distinct mRNA-seq transcriptome profiles. *Int. J. Obes.* **40**, 1452–1460 (2016).
33. V. Sorrentino *et al.*, Enhancing mitochondrial proteostasis reduces amyloid-β proteotoxicity. *Nature* **552**, 187–193 (2017).
34. C. Correia-Melo *et al.*, Mitochondria are required for pro-ageing features of the senescent phenotype. *EMBO J.* **35**, 724–742 (2016).
35. C. D. Wiley *et al.*, Mitochondrial dysfunction induces senescence with a distinct secretory phenotype. *Cell Metab.* **23**, 303–314 (2016).
36. P. A. Williams *et al.*, Vitamin B_3 modulates mitochondrial vulnerability and prevents glaucoma in aged mice. *Science* **355**, 756–760 (2017).
37. Y. S. Lee *et al.*, Increased adipocyte O2 consumption triggers HIF-1α, causing inflammation and insulin resistance in obesity. *Cell* **157**, 1339–1352 (2014).
38. C. Hetz, The unfolded protein response: Controlling cell fate decisions under ER stress and beyond. *Nat. Rev. Mol. Cell Biol.* **13**, 89–102 (2012).
39. R. C. Slieker, C. L. Relton, T. R. Gaunt, P. E. Slagboom, B. T. Heijmans, Age-related DNA methylation changes are tissue-specific with ELOVL2 promoter methylation as exception. *Epigenetics Chromatin* **11**, 25 (2018).
40. S. J. Mitchell, M. Scheibye-Knudsen, D. L. Longo, R. de Cabo, Animal models of aging research: Implications for human aging and age-related diseases. *Annu. Rev. Anim. Biosci.* **3**, 283–303 (2015).
41. C. López-Otín, M. A. Blasco, L. Partridge, M. Serrano, G. Kroemer, The hallmarks of aging. *Cell* **153**, 1194–1217 (2013).